

Efficiency-loss analysis of monolithic perovskite/silicon tandem solar cells by identifying the patterns of a dual two-diode model's current-voltage curves

Yuheng Zeng^{1, 2, 3, †, ‡}, Zetao Ding^{1, 2, 3, †, ‡}, Zunke Liu^{1, 2, 3}, Wei Liu^{1, 3}, Mingdun Liao^{1, 3}, Xi Yang^{1, 2, 3}, Zhiqin Ying^{1, 3}, Jingsong Sun^{1, 3}, Jiang Sheng^{1, 2, 3}, Baojie Yan^{1, 2, 3}, Haiyan He⁴, Chunhui Shou⁴, Zhenhai Yang^{1, 3, †}, and Jichun Ye^{1, 2, 3, †}

¹Ningbo Institute of Materials Technology and Engineering, Chinese Academy of Sciences, Ningbo 315201, China

²University of Chinese Academy of Sciences, Beijing 100049, China

³Zhejiang Engineering Research Center for Energy Optoelectronic Materials and Devices, Ningbo Institute of Materials Technology & Engineering, CAS, Ningbo 315201, China

⁴Zhejiang Energy Group R & D, Hangzhou 310003, China

Abstract: In this work, we developed a simple and direct circuit model with a dual two-diode model that can be solved by a SPICE numerical simulation to comprehensively describe the monolithic perovskite/crystalline silicon (PVS/c-Si) tandem solar cells. We are able to reveal the effects of different efficiency-loss mechanisms based on the illuminated current density-voltage (J - V), semi-log dark J - V , and local ideality factor (m - V) curves. The effects of the individual efficiency-loss mechanism on the tandem cell's efficiency are discussed, including the $\exp(V/V_T)$ and $\exp(V/2V_T)$ recombination, the whole cell's and subcell's shunts, and the Ohmic-contact or Schottky-contact of the intermediate junction. We can also fit a practical J - V curve and find a specific group of parameters by the trial-and-error method. Although the fitted parameters are not a unique solution, they are valuable clues for identifying the efficiency loss with the aid of the cell's structure and experimental processes. This method can also serve as an open platform for analyzing other tandem solar cells by substituting the corresponding circuit models. In summary, we developed a simple and effective methodology to diagnose the efficiency-loss source of a monolithic PVS/c-Si tandem cell, which is helpful to researchers who wish to adopt the proper approaches to improve their solar cells.

Key words: monolithic perovskite/silicon tandem solar cell; efficiency-loss analysis; dual two-diode model; SPICE numerical simulation

Citation: Y H Zeng, Z T Ding, Z K Liu, W Liu, M D Liao, X Yang, Z Q Ying, J S Sun, J Sheng, B J Yan, H Y He, C H Shou, Z H Yang, and J C Ye, Efficiency-loss analysis of monolithic perovskite/silicon tandem solar cells by identifying the patterns of a dual two-diode model's current-voltage curves[J]. *J. Semicond.*, 2023, 44(8), 082702. <https://doi.org/10.1088/1674-4926/44/8/082702>

1. Introduction

A tandem cell that has the ability to fully use solar spectrum energy is considered as a promising solar-cell technology because it enables an efficiency beyond the single-junction solar cell. Detailed-balance theory predicts that the up-limit efficiency of a tandem cell can reach 42%^[1], which far exceeds the 30% up-limit efficiency of a single-junction cell^[2, 3]. A tandem solar cell consisting of a perovskite (PVS) thin-film top cell and a crystalline-silicon (c-Si) bottom cell has attracted attention in the past few years because it can balance high efficiency and low cost. The prediction of the practical efficiency of this kind of tandem cell is higher than 30%^[4, 5]. The latest world record of monolithic PVS/c-Si tandem cells has reached 32.5%^[6], which has surpassed the efficiency limit of a practical single-junction c-Si solar cell (i.e., 27%–28%)^[7, 8].

Developing the high-performance monolithic PVS/c-Si is of great importance for photovoltaic study.

The monolithic PVS/c-Si tandem cell, including two sub solar cells and one intermediate layer, usually involves nearly 20 functional layers and dozens of fabrication steps. Therefore, inappropriate processes or unexpected damage will lead to degradation of the cell's performance. However, it is difficult to identify the reason for efficiency loss when only using an illuminated current density-voltage (J - V) curve. With the help of the characterization of materials and layers, one may identify the efficiency loss. However, most of these methods are destructive or ex-situ, which cannot describe the whole picture of efficiency loss. As a result, the lack of a direct, simple, and effective analysis method is still a block for developing a high-efficiency tandem cell.

An electrical analysis that is damage-free, easy handling, and high reliability would be an ideal method for identifying efficiency loss. The J - V curve analysis built on Shockley's ideal diode model is a standard and effective method for diagnosing the efficiency loss of c-Si solar cells^[9]. With development, the two-diode model has been widely employed to describe the illuminated and dark current-voltage curves of c-Si solar cells^[10]. The corresponding semi-log dark J - V curve and dark

Yuheng Zeng and Zetao Ding contributed equally to this work and should be considered as co-first authors.

Correspondence to: Y H Zeng, yuhengzeng@nimte.ac.cn; Z H Yang, yangzhenhai@nimte.ac.cn; J C Ye, jichun.ye@nimte.ac.cn

Received 17 FEBRUARY 2023; Revised 24 MARCH 2023.

©2023 Chinese Institute of Electronics

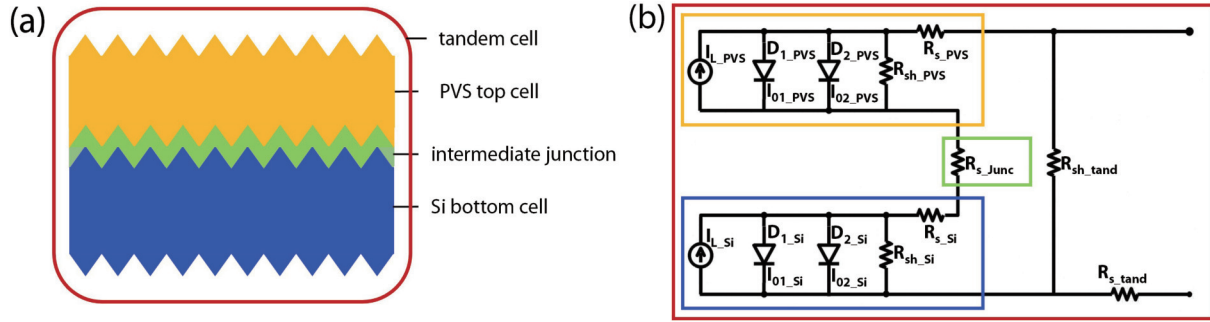


Fig. 1. (Color online) (a) Schematic diagram and (b) diode model of the perovskite/Si tandem solar cell. Note that a well-fabricated intermediate junction is considered as a resistor; alternatively, an improperly prepared intermediate junction is considered as a Schottky junction.

local ideality factor (m) vs voltage (m - V) curve are effective tools to diagnose the efficiency-loss mechanism^[11]. However, few studies have used the diode model to analyze PVS/Si tandem cells. Several existing works that have discussed the circuit model for PVS/Si tandem cells have focused on establishing a more reliable analytic formula for understanding the physical mechanism but do not provide a guideline for diagnosing a tandem cell^[12, 13]. The subcells and intermediate layer were studied separately by Lang *et al.*^[14] and Agarwal *et al.*^[15] respectively, but a whole view of tandem cell is not available. A numeric model of the whole tandem cell was proposed by Blaga *et al.*, but their model is complicated and still has some shortages^[16]. Developing an analysis tool to determine the efficiency-loss source is of critical importance for taking further steps to improve the cell's efficiency.

In this work, we employ a circuit model with dual two-diode models in series to describe the monolithic PVS/c-Si tandem solar cells. As mentioned earlier, a two-diode model has been used to simulate a silicon solar cell^[10]. For perovskite solar cells, many studies prove that a well-fabricated perovskite cell can eliminate hysteresis or S-shape and behave like inorganic semiconductors, which can be also described using a two-diode model^[17-21]. Therefore, dual two-diode models in series may be reliable. This work aims to investigate the features of J - V and m - V curves of a PVS/c-Si tandem cell to reveal the possible loss mechanisms of tandem cell efficiency and to provide guidance for cell improvement. In addition, we employ the numerical circuit simulator built on SPICE (Simulation Program with Integrated Circuit Emphasis) code to solve the tandem cells' illuminated and dark J - V curves, which may offer a particular group of parameters from fitting practical J - V curves but avoids complicated analytic formula. Furthermore, this circuit model can serve as an open platform for analyzing other kinds of tandem solar cells by substituting the corresponding electrical models.

2. Models and analysis methods

The two-diode model is used to describe the perovskite and c-Si subcells. The analytic formula of a typical two-diode model is given in Eq. (1). Note that I and V represent the current and voltage, respectively; I_L is the photogenerated current; V_T is thermal voltage ($V_T = kT/q$); k is Boltzmann constant; q is the charge of an electron; R_{sh} is the shunt resistor; R_s is the series resistor; D_1 (D_2) represents the diode with the ideal factor of 1 (2); I_{01} (I_{02}) is the dark saturation current of the diode D_1 (D_2).

$$I = I_L - I_{01} \exp\left(\frac{V + IR_s}{V_T}\right) - I_{02} \exp\left(\frac{V + IR_s}{2V_T}\right) + \frac{V + IR_s}{R_{sh}}. \quad (1)$$

The parameters of a two-diode model typically represent different kinds of Shockley-Read-Hall (SRH) recombination mechanisms. This understanding holds for various types of semiconductor devices, such as Si solar cells and PVS solar cells, because the SRH recombination mechanism of a diode model is deduced from semiconductor physics. For example, the $\exp(V/V_T)$ item is coherent with the recombination when one kind of carrier concentration is much higher than the other. This recombination typically occurs in the surface or bulk zone where two carrier concentrations differ significantly. Thus, the parameter I_{01} corresponding to $\exp(V/V_T)$ recombination indicates the degree of surface or bulk recombination^[22]. The $\exp(V/2V_T)$ item with the corresponding parameter I_{02} reflects the recombination when the concentrations of electron and hole are comparable. This SRH recombination typically happens in the depletion region^[23], at an edge zone^[24], or under high injection condition^[9]. R_{sh} reflects the extent of current leakage, while R_s is the sum of internal resistance^[25].

The PVS/c-Si tandem cell consists of two subcells that are connected by an intermediate junction, whose model is shown in Fig. 1(a). The corresponding circuit model is displayed in Fig. 1(b). For a clear discussion, we have defined all of the components in the circuit. The circuit components in the Si subcell are defined as D_{1_Si} , D_{2_Si} , R_{sh_Si} and R_{s_Si} respectively, where D and R represent the diode and resistor, the subscript numbers 1 and 2 represent the corresponding ideal factor of a diode, and the subscript Si denotes that the component belongs to the Si subcell.

According to Kirchhoff's current law, the total circuit current is the sum of the currents from all the branches. In our model, the current flows through three different paths of the Si bottom subcell, i.e., D_{1_Si} , D_{2_Si} and R_{sh_Si} ; at the same time, and the current flows through another three paths of the PVS top subcell, i.e., D_{1_PVS} , D_{2_PVS} , and R_{sh_PVS} . Thus, it produces nine different branches when the current goes through the top and bottom cells. It then becomes 10 branches for a tandem cell if plus the R_{sh_tand} path. The branch is defined by the corresponding components where current flows, e.g., the branch D_{1_Si} - D_{1_PVS} represents that the current goes through both the D_{1_Si} and D_{1_PVS} components. According to the differences in the circuit components, the 10 branches can be divided into three categories. The first category contains only resistors, including R_{sh_tand} and R_{sh_Si} - R_{sh_PVS} ; the second category contains both resistors and diodes, including D_{2_Si} - R_{sh_PVS} ,

Table 1. Default parameters used for the tandem solar cell.

	I_{01} (A/cm ²)	I_{02} (A/cm ²)	R_{sh} (Ω·cm ²)	R_s (Ω·cm ²)	J_L/J_{sc} (mA/cm ²)	V_{oc} (mV)	FF (%)	PCE (%)	MPP (mV)
Si subcell	6×10^{-14}	5×10^{-9}	1×10^5	0.2	41.5	702	82.0	24.0	608
PVS subcell	1×10^{-21}	1×10^{-11}	3×10^3	0.4	21.5	1096	80.0	19.0	943
Junction				0.01					
Tandem			1×10^5	0.1	19.5	1781	82.0	28.5	1535

$R_{sh_Si-D_{2_PVS}}$, $D_{1_Si}-R_{sh_PVS}$, and $R_{sh_Si}-D_{1_PVS}$; the third category contains only diodes, including $D_{2_Si}-D_{2_PVS}$, $D_{2_Si}-D_{1_PVS}$, $D_{1_Si}-D_{2_PVS}$, and $D_{1_Si}-D_{1_PVS}$.

The numerical simulator built on SPICE is used to solve the circuit model and depict the illuminated or dark J - V curves. With the help of the SPICE simulator, we can study the electrical behavior of the tandem cells:

1) By altering the parameters of each component, we can investigate the influences of different efficiency-loss mechanisms on the J - V curves. This topic is discussed in this paper.

2) By looking for the parameters to produce the simulated J - V curves to fit a practical one, we can find specific groups of parameters approaching an objective tandem cell. We can then make an accurate diagnosis for efficiency loss through a comprehensive analysis of the device structure, experimental process, and fitted parameters. The second topic is not discussed herein.

To examine the method's reliability, we carry out a calculation by referring to a practical tandem cell. The monolithic PVS/c-Si tandem solar cell's parameters are extracted from the laboratory achievable ~24%-efficiency c-Si solar cell^[26], ~19%-efficiency semi-transparent perovskite thin-film solar cell^[27], and the 28.2% PVS/c-Si tandem cell^[28], as listed in Table 1. These parameters are also used as the default parameters for the tandem cell in the whole work. The illuminated J - V curves of the c-Si and perovskite solar cells are well reproduced by the numerical simulation, which proves the reliability of the model and parameters; as shown in Fig. 2(a). In addition, the parameters of the intermediate recombination junction are referred to our previous work^[29], which shows Ohmic characteristics with a series resistance of ~0.02 Ω·cm². It is assumed that the tandem cell, by default, has no leakage with a R_{sh_tand} of 100000 Ω·cm² and a small additional internal series resistance of 0.1 Ω·cm². The photogenerated current densities of the perovskite top cell and the c-Si bottom cell are assumed as 20 mA/cm² and 19.5 mA/cm², respectively. The illuminated J - V curve of the tandem cell is produced with an efficiency of 28.5%, as shown in Table 1. The parameters of the single-junction c-Si solar cell and perovskite thin-film solar cell are given as a reference in Table 1. The calculated results match our actual tandem and single-junction solar cells^[26-28], which proves that the method is reliable.

In this work, we focus on the effects of critical parameters on the J - V curves of tandem cells. The dark J - V curve is used as the indicator of efficiency loss sources because it is a better choice than the illuminated one by eliminating the light source fluctuations. The dark J - V curve is re-plotted as the semi-logarithm (semi-log) J - V curve and the local ideality factor verse voltage (m - V) curve to discover the subtle current change in the J - V curve and amplify the characteristics of the J - V curve, respectively. The local ideality factor (m) represents the extent of carrier recombination happens in a practical

diode vs an ideal diode. A higher m implies a higher recombination rate^[11, 30, 31]. The m is calculated from Eq. (2), where m is a dimensionless value.

$$m = \frac{1}{V_T} \left[\frac{dV}{d(\ln I)} \right] = \frac{I}{V_T} \frac{dV}{dI}. \quad (2)$$

The main contents of this work include:

1) The features of semi-log dark J - V and m - V curves of the individual circuit branch;

2) The effects of the bottom subcell's V_{oc} loss, originated from the $\exp(V/V_T)$ and $\exp(V/2V_T)$ recombination, on the performance of the tandem cell;

3) The effects of shunt leakage, originated from a tandem cell or a subcell, on the performance of the tandem cell;

4) The influence of the intermediate junction, including both Ohmic-contact and Schottky-contact type, on the performance of the tandem cell.

3. Results and discussion

3.1. Mechanisms of efficiency loss

Figs. 2(a) and 2(b) show the illuminated and dark J - V curves of the tandem cell (in red), c-Si single-junction cell (in blue), and perovskite single-junction cell (in yellow), respectively, which are depicted using the default parameters listed in Table 1. The tandem cell shows an efficiency (η) of 28.47% with an open-circuit voltage (V_{oc_tand}) of 1780 mV, a short-circuit current density (J_{sc_tand}) of 19.51 mA/cm², a fill factor (FF_tand) of 81.95%, and a maximal power point (MPP_tand) at 1535 mV. The V_{oc_tand} of the tandem cell is the sum of the subcells' V_{oc} .

To find the efficiency-loss mechanisms, we plot the semi-log dark J - V curve of the tandem cell and the ten branches in Fig. 2(c). The following observations are found:

1) The three different kinds of branches show individual characteristics in the semi-log dark J - V curve. The branch containing only shunt resistors shows a rounded characteristic on the semi-log longitudinal coordinates. The branches containing only diodes show a straight line whose slope depends on the sum of the diode's ideal factors. The branches containing resistor and diode show diode characteristics typically at low voltage region and shunt characteristics at high voltage region.

2) The semi-log dark J - V curve of the total circuit is dominated by different branch currents in different voltage ranges. For example, the branches containing only resistors dominate in the low-voltage region, those containing both resistors and diodes dominate in the medium voltage region, and those containing two diodes tend to dominate in the high voltage region. The current starts to flow through the resistor under low voltage and grows linearly with voltage, and then the current can flow through the diode under turn-on voltage and grows exponentially with voltage. The smaller

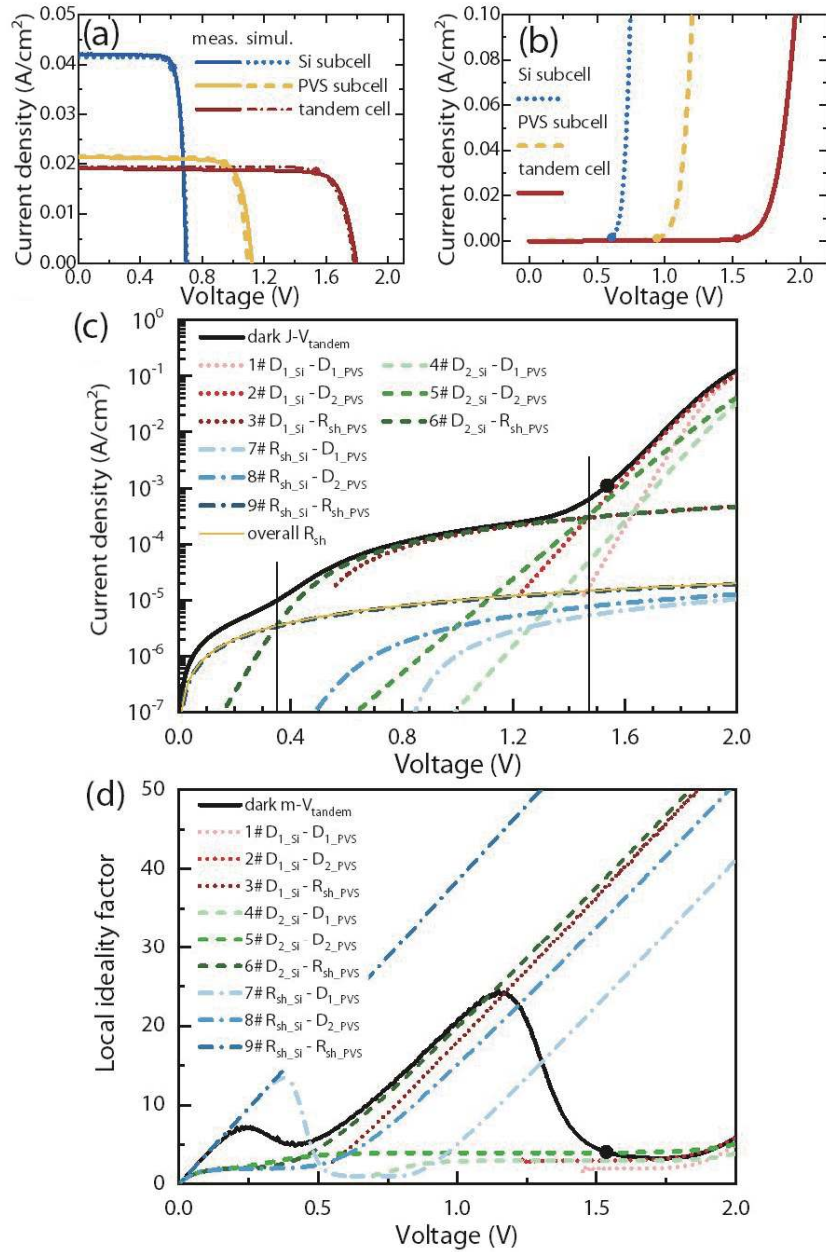


Fig. 2. (Color online) (a) Illuminated J - V curves, (b) dark J - V curves of the 24% Si solar cell, 19% PVS solar cell, and 28.5% PVS/Si tandem solar cell, which parameters listed in Table 1 are extracted from the reported Si and perovskite solar cells. (c) Semi-log dark J - V curves and (d) m - V curves of the 28.5% PVS/Si tandem solar cell and the individual branches from the diode models.

the saturation current density of a diode indicates a higher turn-on voltage and a more significant growth with voltage.

3) The tandem cell's semi-log dark J - V curve overlaps with the dominated branch's curve, reminding us that one can find the dominated branch from the shape of the semi-log J - V curve. The branches R_{sh_tand} and $R_{sh_Si}-R_{sh_PVS}$ dominate about 0–0.34 V; the branch $D_{2_Si}-R_{sh_PVS}$ dominates about 0.34–1.46 V; the branch $D_{2_Si}-D_{2_PVS}$ dominates about 1.46–1.49 V; finally, the branch $D_{1_Si}-D_{2_PVS}$ dominates >1.49 V.

The m - V curves are shown in Fig. 2(d), and we find the following observations:

- 1) The branches containing only resistors show a linear growth of m with voltage.
- 2) The branches containing both resistor and diode show a constant m value in the low or low-to-intermediate voltage range, where the m value is the sum of the diode's ideal factors. The m value grows linearly with voltage in the high volt-

age and other voltage ranges.

3) The branches containing only diodes display a constant m value in intermediate-to-high voltage. The m value grows quickly at the high voltage, which can be attributed to the effect of the series resistor.

4) Similar to the pattern presented by the semi-log dark J - V curve, the tandem cell's m - V curve tends to overlap with one of the dominant branches, which helps us to identify the dominating branch typically representing the efficiency loss for the cells.

The dominant recombination loss at MPP mainly comes from the dominating branch^[11]; thereby, identifying the dominant branch at MPP allows us to lock the primary recombination loss of the cell and look for solutions to improve the cells. Ideally, the MPP point of a high-efficiency solar cell should be located at the lowest point of the m - V curve, typically dominated by the branches with only D_1 diodes, mean-

Table 2. The setting I_{01_Si} and I_{02_Si} values of the Si subcells.

	600 mV	640 mV	670 mV	700 mV	730 mV
I_{01_Si} (A/cm ²)	3.4×10^{-12}	7×10^{-14}	2.2×10^{-13}	6×10^{-14}	2×10^{-14}
I_{02_Si} (A/cm ²)	3.7×10^{-7}	1.6×10^{-7}	7.2×10^{-8}	5×10^{-9}	1×10^{-11}

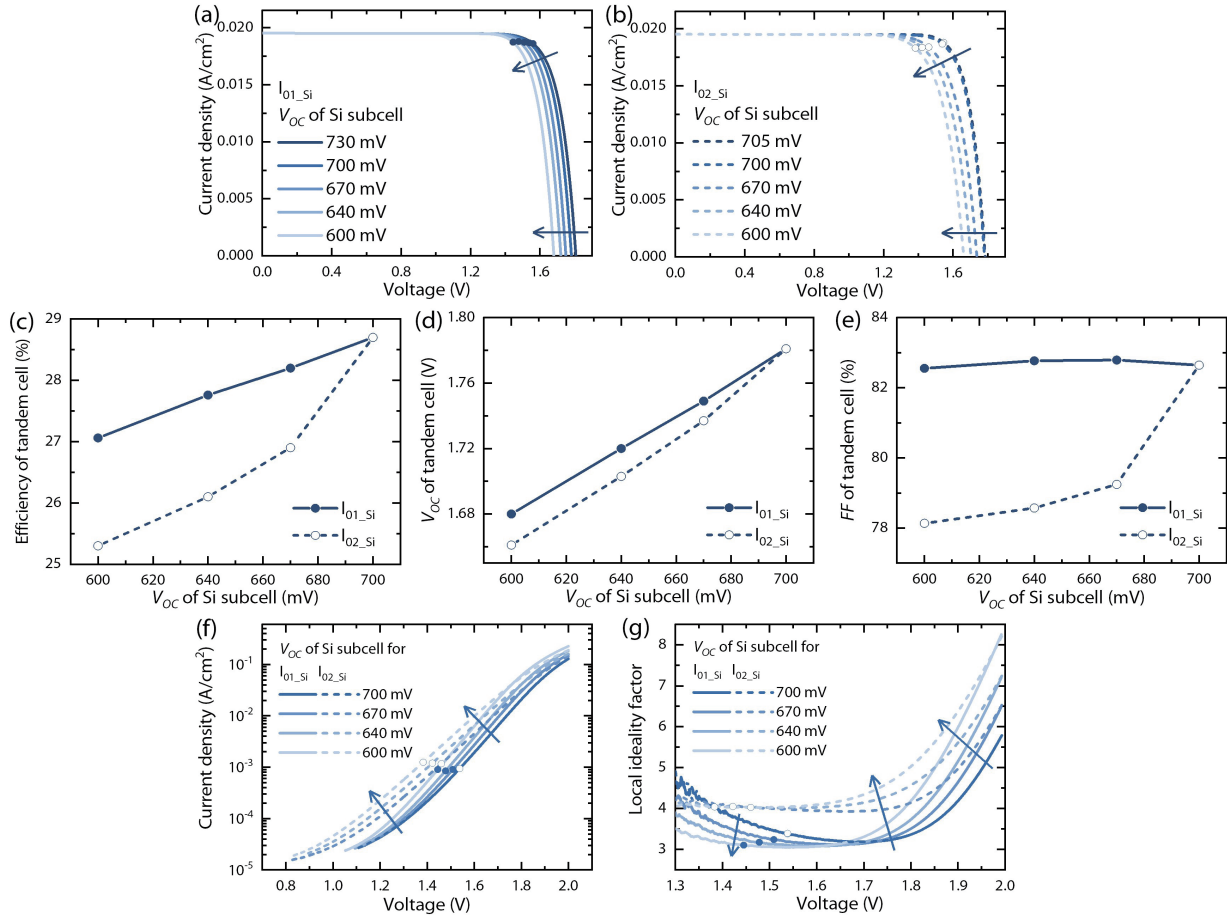


Fig. 3. (Color online) Illuminated J - V curves of the PVS/Si tandem cells whose efficiency loss is originated from the different Si subcell's V_{oc} -loss mechanisms, *i.e.*, (a) I_{01_Si} and (b) I_{02_Si} , respectively. Effects of I_{01_Si} and I_{02_Si} on (c) the efficiency, (d) the V_{oc} , (e) the FF , (f) the semi-log dark I - V curves, and (g) the m - V curves of the tandem cells.

ing that the dominating SRH recombination is only the bulk or surface recombination. For the tandem cell in this work, as shown in Fig. 2(c) and 2(d), MPP at 1535 mV is mainly determined by the branch D_{1_Si} - D_{2_PVS} , indicating that the primary efficiency loss comes from the recombination of D_{1_Si} or D_{2_PVS} .

3.2. Effects of SRH recombination

The $\exp(V/V_T)$ or $\exp(V/2V_T)$ SRH recombination will lower the subcell's V_{oc} , eventually leading to efficiency loss of the tandem cell. How to distinguish the type of $\exp(V/V_T)$ or $\exp(V/2V_T)$ recombination from the semi-log dark J - V curve and m - V curves is essential to diagnose the efficiency loss. The effects of the two kinds of recombination in Si bottom subcell on the tandem cell's performance are discussed as an example to demonstrate this issue. I_{01} or I_{02} is used to mark the carrier recombination happened under large or tiny difference between electron and hole concentrations. The impact of two kinds of recombination towards Si subcell is presented by Si subcell V_{oc} .

For a clear comparison of the influences from I_{01} and I_{02} , we adjust the I_{01_Si} and I_{02_Si} values, making the V_{oc} of the Si

subcell 730, 700, 670, 640, and 600 mV, respectively. The corresponding I_{01_Si} and I_{02_Si} are given in Table 2. The illuminated J - V curves, η , V_{oc} , and FF of the tandem cells are plotted in Figs. 3(a)–3(e). The I_{02_Si} results in a more severe efficiency loss in the tandem solar cell than the I_{01_Si} , when the Si subcells have the same V_{oc} . Figs. 3(d) and 3(e) show that, compared with V_{oc} loss, the efficiency loss caused by I_{02_Si} is primarily the FF loss. This suggests that $\exp(V/2V_T)$ recombination has more pronounced impacts on current on MPP and leads to a significant drop in FF .

To further compare the effects between I_{01_Si} and I_{02_Si} , the semi-log J - V and m - V curves associated with the Si subcells from 600 mV to 700 mV are given in Figs. 3(f) and 3(g). In the semi-log J - V curve, the significant increase of I_{02_Si} curves happens at the lower voltage range than the counterpart I_{01_Si} ones. The dark current density of the I_{02_Si} curve is higher than the counterpart I_{01_Si} by several times at MPP. This means I_{02} recombination is more remarkable than the I_{01} recombination, which may be the primary loss mechanism. In the m - V curve, the I_{02_Si} leads to a prolonged and lower dominant voltage range. The I_{01_Si} curve dominates in 1.4–1.7 V, while the I_{02_Si} one dominates in 1.2–1.65 V. Moreover, the m

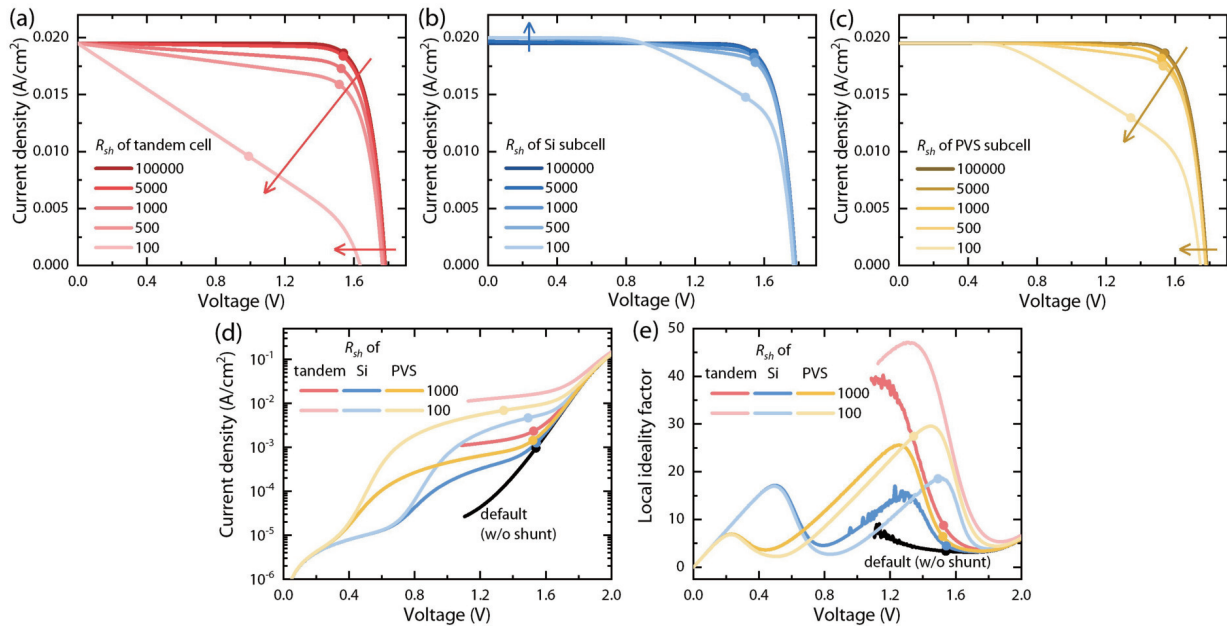


Fig. 4. (Color online) Illuminated J - V curves of the PVS/Si tandem cells with different shunt resistances originated from (a) the full cell, (b) the Si subcell, or (c) the PVS subcell. The shunt resistance values are set as 100000, 5000, 1000, 500, and 100 $\Omega\cdot cm^2$, representing different degrees of leakage. The semi-log dark J - V curve comparison (d) and m - V curve comparison (e) of the three cells with shunt resistances of 1000 and 100 $\Omega\cdot cm^2$.

value of the I_{01_Si} curve's MPP is ~ 3 , while the m value of the I_{02_Si} curve's MPP is ~ 4 , which suggests a more severe recombination in I_{02_Si} case. Therefore, when the V_{oc} loss from the Si subcell is the same, the $\exp(V/2V_T)$ recombination leads to more efficiency loss than the $\exp(V/V_T)$ recombination. This understanding should also be applicable to the PVS top cell.

3.3. Effects of shunt loss

A shunt resistor causing current leakage is one of the common phenomena for efficiency loss. However, the shunt in tandem cells is more complicated because the current leakage may come from the whole cell, PVS top cell, or Si bottom cell. Therefore, determining how to tell the source of leakage accurately is instructive for diagnosing a tandem cell. To illustrate this issue, we set the shunt resistor as 100 000, 5000, 1000, 500, and 100 $\Omega\cdot cm^2$, respectively, for the tandem cell (R_{sh_tand}), PVS top cell (R_{sh_PVS}), and the c-Si bottom cell (R_{sh_Si}).

The illuminated J - V curve, semi-log dark J - V curve, and m - V curves are shown in Fig. 4. We can obtain the following observations from Figs. 4(a)–4(c):

1) If a shunt occurs in the whole cell, then the slope of the illuminated J - V curve starts to decline from zero voltage. The slope decline becomes significant with the decrement of R_{sh_tand} , which degrades the FF first, and finally, the V_{oc} if R_{sh_tand} is reduced continuously. The characteristics of the illuminated J - V curve caused by the tandem cell are similar to that of a single-junction c-Si cell^[22].

2) If a shunt occurs in the Si or PVS subcell, then the shape of the illuminated J - V curve shows different features from the one belonging to the whole cell, *i.e.*, the decrease of the J - V curve's slope does not occur from zero voltage but a specific voltage. With the decrease of shunt resistance, the FF and finally the V_{oc} fall. It seems that the degree of FF decrement of a subcell is smaller than the whole cell's case with the same shunt resistance.

3) The degree of efficiency loss is more severe in PVS sub-

cell than in the Si one with the same shunt resistance. This may indicate that a PVS top cell with low shunt current is more important for a tandem cell.

Furthermore, to distinguish the difference between the leakage of the top and bottom cells, we plot the semi-log dark J - V curves and m - V curves; as shown in Figs. 4(d) and 4(e). In the semi-log J - V curves, the remarkable increment of dark current occurs from a small voltage in the PVS subcell, and the dark current density is larger than the Si subcell for the same shunt resistance. In the m - V curves, the PVS shunt dominates the m - V from ~ 0.5 V to the higher voltage, while the Si shunt dominates from ~ 0.8 V to the higher voltage. The PVS shunt dominates a broader voltage range than the Si one. The fact that the PVS subcell possesses small D_{1_PVS} and D_{2_PVS} diode saturation current density than the Si counterpart means that the branch containing the PVS subcell diode has a higher turn-on voltage, which helps to suppress the leakage current from the top cell. On the contrary, the Si subcell has a weaker capability to suppress the leakage from the top cell. Thus, if the shunt resistances are the same in the subcell, the PVS's shunt will cause more severe efficiency loss. Therefore, identifying the shunt originated from the top or bottom cell is, in principle, effective by examining the beginning of shunt dominating voltage. Typically, if the shunt starts to dominate from low voltage, *e.g.*, ~ 0.5 V, then it may suggest the leakage from the PVS subcell; and vice versa, *e.g.*, ~ 0.8 V, maybe from the Si subcell.

We can find that the degree of FF decrement of a subcell is smaller than the whole cell's case with the same shunt resistance. The reason for this can be addressed as follows. The perovskite subcell and silicon subcell are connected in series. If the PVS subcell leaks, then the leakage current will still pass through the Si subcell; thus, the leakage current is suppressed by the Si subcell and its effect on FF is limited. In comparison, if the leakage occurs on the whole cell, *i.e.*, the leakage current pass only through R_{sh_tand} without limit, then

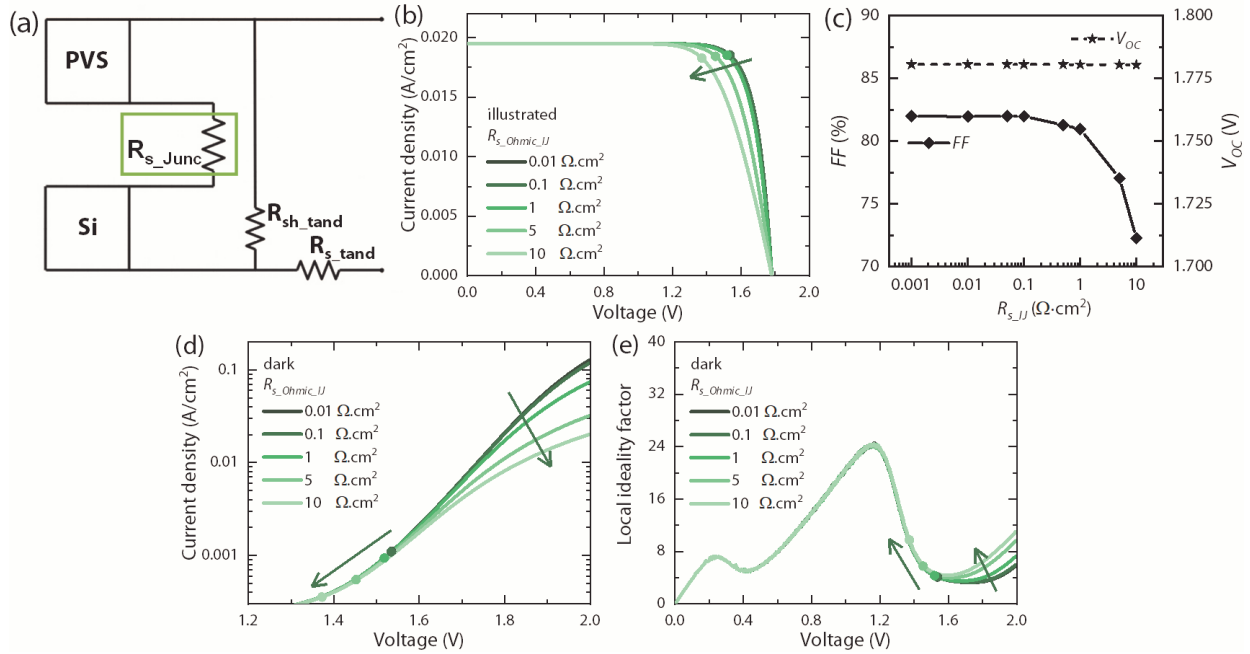


Fig. 5. (Color online) (a) Schematic diagrams of the Ohmic-contact intermediate junction. Effects of the intermediate junction with different resistances on (b) the illuminated J - V curves, (c) the V_{oc} and FF , (d) the semi-log dark J - V curves, and (e) the m - V curves.

this makes a much more significant decrement in FF .

3.4. Effects of intermediate junction

The intermediate junction as the connection between the top and bottom cell is critical for the performance of the tandem cell. In principle, a well-fabricated intermediate junction should be an Ohmic-contact resistor that enables the electron and hole to transport by tunneling from the top and bottom cells, and then recombine entirely in the junction. Thus, the intermediate junction is also called a tunnel junction (TJ), recombination junction (RJ), or tunnel-recombination junction (TRJ). However, an intermediate junction that is fabricated improperly may become a Schottky junction with a reverse rectification function. Both the Ohmic-contact type and Schottky-contact type intermediate junctions are investigated herein.

3.4.1. Ohmic-contact intermediate junction

We first investigate the effects of the Ohmic-contact type intermediate junction on the efficiency of tandem cells. The resistances of the intermediate junction (R_{s_IJ}) are set as 0.001, 0.01, 0.05, 0.1, 0.5, 1, 5, and 10 $\Omega\cdot\text{cm}^2$, respectively. As shown in Fig. 5(a), the Ohmic-contact type intermediate junction works like a series resistor from the view of the circuit model.

As indicated by the illuminated J - V curves, the effects of the intermediate junction with a resistance below 0.1 $\Omega\cdot\text{cm}^2$ on the tandem cells are negligible. The efficiency loss starts to become visible as the resistance becomes more than 1 $\Omega\cdot\text{cm}^2$, where the FF decreases to 80.95%, 77.05%, and 72.21%, with the corresponding resistances of 1, 5, and 10 $\Omega\cdot\text{cm}^2$, respectively. The effects of the intermediate junction's resistance on efficiency loss are revealed more clearly by plotting the semi-log dark J - V and m - V curves. As indicated by the semi-log dark J - V curve, the effects of the intermediate junction's resistance on MPP are limited because the resistance is smaller than 1 $\Omega\cdot\text{cm}^2$. This observation also holds in the m - V curves. If the R_{ohm_IJ} becomes large enough, e.g.,

5 $\Omega\cdot\text{cm}^2$, the intermediate junction dominating region extends to the voltage where MPP locates, which lowers the FF of the tandem solar cells.

This observation indicates that the tandem solar cells possess a much higher tolerance to series resistance than the Si solar cell. This deduction is reasonable because the photogenerated current of the tandem cell is significantly lower than that of the Si cell, leading to a smaller power loss on the resistor. Thus, the influence of an intermediate junction with a resistance of $<0.5 \Omega\cdot\text{cm}^2$ is small for a tandem cell, whose resistance is easily achievable for a well-fabricated intermediate junction.

3.4.2. Schottky-contact intermediate junction

An improperly fabricated intermediate junction may become a Schottky junction with a reverse rectification effect. The saturation current density ($I_{0_Schottky_IJ}$) is the essential parameter to determine the turn-on voltage; thus, a series of $I_{0_Schottky_IJ}$, including 1, 0.01, 1×10^{-4} , 1×10^{-6} , 1×10^{-8} A/cm², are considered in the following simulation. Figs. 6(a)-6(e) show the effects of the Schottky saturation current density on the illuminated J - V curves.

As shown in Figs. 6(b) and 6(c), the effects of the Schottky-type intermediate junction on the efficiency are limited when the $I_{0_Schottky_IJ}$ of ≥ 0.1 A/cm². The effects on the efficiency loss start to become pronounced with an $I_{0_Schottky_IJ}$ of ≤ 0.01 A/cm². If the effects of Schottky-type intermediate junction with an $I_{0_Schottky_IJ}$ of ≤ 0.0001 A/cm² become particularly severe, then the illuminated J - V curve will not intersect with the X-axis. In such cases, the FF and the efficiency of the tandem solar cell degrade significantly. If the saturation current density decreases further, then FF and the efficiency decrease further and rapidly.

The Schottky-contact intermediate junction shows unique and remarkable features in the semi-log J - V curve and m - V , as presented in Figs. 6(d) and 6(e). The dark current density in the semi-log J - V plot will no longer increase with volt-

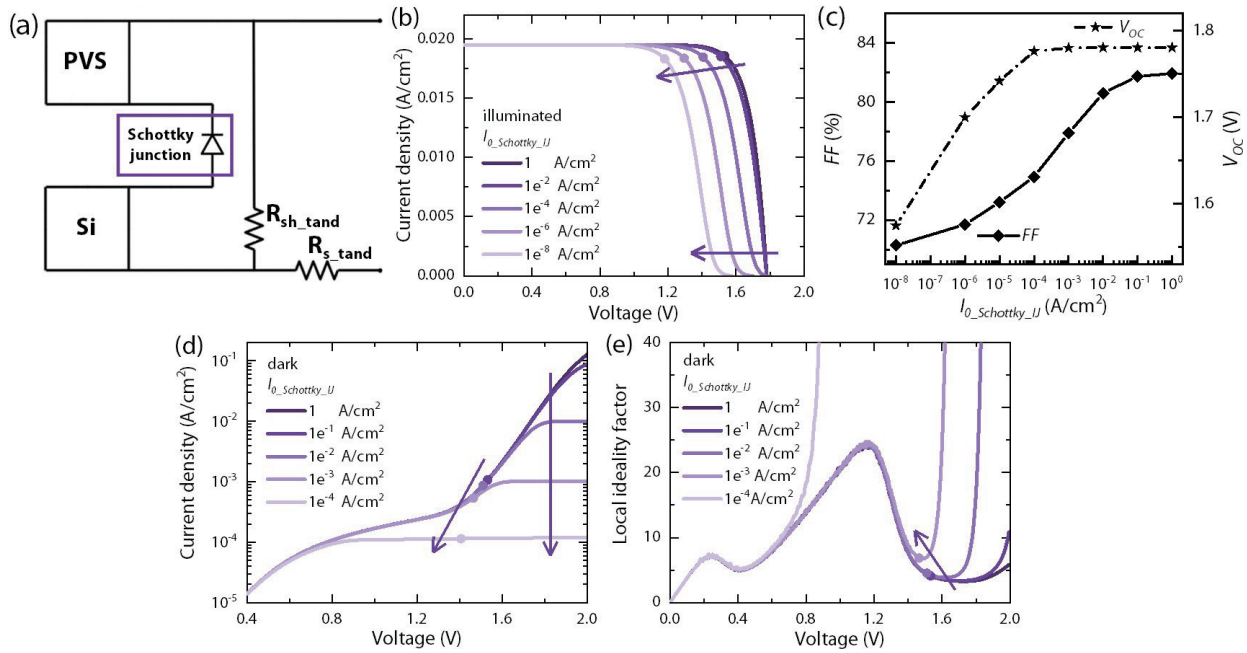


Fig. 6. (Color online) (a) Schematic diagrams of the Schottky-contact intermediate junction. Effects of the intermediate junction with different saturation current densities on (b) the illuminated J - V curves, (c) the V_{oc} and FF , (d) the semi-log dark J - V curves, and (e) the m - V curves.

age after a specific voltage if the $I_{0_Schottky_IJ}$ is decreased to ≤ 0.01 A/cm², which should be attributed to the reverse cut-off effect of the Schottky junction. The reverse cutoff dominating zone extends to a lower voltage range with decreasing $I_{0_Schottky_IJ}$. For the m - V curve, the effect of the Schottky-contact intermediate junction is not visible when the $I_{0_Schottky_IJ}$ is more than 0.1 A/cm². However, when the $I_{0_Schottky_IJ}$ becomes less than 0.01 A/cm², the m value will rise steeply at a specific voltage, behaving like a vertical line. If the $I_{0_Schottky_IJ}$ is reduced further, then the Schottky-junction dominating zone is shifted toward the lower voltage region, and the m value rises steeply from a lower voltage. It is easy to distinguish a Schottky-type intermediate junction from its unique and remarkable features in the illuminated J - V , semi-log dark J - V curve, and m - V curve.

3.5. Others

The method that is provided in this work can also be used to fit the J - V curves of a practical tandem cell. Although the fitting J - V curves could be different combinations of parameters, *i.e.*, the fitting parameters are not a unique solution, they are still valuable clues for diagnosing the cells with the aid of cell design and experimental processes. This method helps researchers to identify the efficiency loss and take steps to improve the performance of the tandem solar cells. Furthermore, this method also serves as an open platform. By substituting new circuit models, other kinds of tandem solar cells can be described, *e.g.*, GaAs/Si and perovskite/CIGS, which improves the method's versatility.

4. Conclusion

In this work, we developed a circuit model with dual two-diode models in series to describe the monolithic PVS/c-Si tandem solar cells and we used a SPICE numerical simulation to study the relationship between the efficiency-loss mechanism and J - V curves, as well as m - V curves. The effects of various recombination mechanisms, including the

$\exp(V/V_T)$ and $\exp(V/2V_T)$ recombination, whole cell's and sub-cell's shunt, and intermediate junction, on the efficiency loss are discussed. A summary follows:

1) A tandem cell is a superposition of 10 different circuit branches representing the unique efficiency-loss mechanism. In general, the semi-log dark J - V curve or the m - V curve of the tandem cell tends to display the feature of the dominated branch. The efficiency loss at MPP is mainly caused by the recombination belonging to the dominant branch. Therefore, identifying the dominant branch at MPP allows us to lock the primary recombination loss and take steps to improve the cells.

2) If the $\exp(V/V_T)$ recombination ($I_{01_subcell}$) and $\exp(V/2V_T)$ recombination ($I_{02_subcell}$) lead to the same subcell's V_{oc} , then the degree of efficiency loss of the tandem cell is quite different. The $\exp(V/2V_T)$ item typically representing depletion or edge recombination causes much more significant efficiency loss than the $\exp(V/V_T)$ one representing surface or bulk recombination.

3) The subcell's and whole cell's leakage show different features in the illuminated J - V curves. The whole cell's leakage shows a similar illuminated J - V curve to the single-junction cell. However, the subcell's leakage shows an illuminated J - V curve, whose slope decreases not from zero voltage but a specific voltage. Typically, if the shunt starts to dominate from a low voltage, *e.g.*, ~ 0.5 V, then it probably suggests the PVS subcell's leakage; and vice versa, maybe from the Si subcell, *e.g.*, ~ 0.8 V.

4) The Ohmic-contact intermediate junction behaves like a series resistance, which is challenging to identify. Generally, an Ohmic-contact intermediate junction's effects on efficiency are possibly limited because a tandem cell possesses high tolerance to series resistance. Schottky-type intermediate junction with reverse rectification effect can be easily distinguished by the unique and visible features. In such a case, the effects of a Schottky-type intermediate junction on the efficiency are significant and damaging.

Besides revealing the effects of various efficiency loss mechanisms, we can also fit a practical J - V curve and find a specific group of parameters by the trial-and-error method. Although the fitted parameters are not a unique solution, they are valuable clues for identifying the efficiency loss with the aid of the cell's structure and experimental processes. This method can also serve as an open platform for analyzing other tandem solar cells by substituting the corresponding circuit models. In summary, we have developed a simple and effective tool to diagnose the efficiency-loss sources of a monolithic PVS/c-Si tandem cell, which is helpful to researchers who wish to adopt proper approaches to improve their solar cells.

Acknowledgements

This work was supported by Zhejiang Energy Group (zknj-2018-118), Key Research and Development Program of Zhejiang Province (2021C01006), Key Project of Zhejiang Province (2021C04009), Science and technology projects in Liaoning Province 2021 (2021JH1/10400104), Ningbo "Innovation 2025" Major Project (2020Z098), National Key R&D Program of China (2018YFB1500403), National Natural Science Foundation of China (61974178, 61874177, 62004199), and Youth Innovation Promotion Association (2018333).

References

- [1] De Vos A. Detailed balance limit of the efficiency of tandem solar cells. *J Phys D: Appl Phys*, 1980, 13, 839
- [2] Shockley W, Queisser H J. Detailed balance limit of efficiency of p-n junction solar cells. *J Appl Phys*, 1961, 32(3), 510
- [3] Schäfer S, Brendel R. Accurate calculation of the absorptance enhances efficiency limit of crystalline silicon solar cells with lambertian light trapping. *IEEE J Photovolt*, 2018, 8(4), 1156
- [4] Bremner S P, Levy M Y, Honsberg C B. Analysis of tandem solar cell efficiencies under AM1.5G spectrum using a rapid flux calculation method. *Prog Photovolt*, 2008, 16(3), 225
- [5] Shen H P, Walter D, Wu Y L, et al. Monolithic perovskite/Si tandem solar cells: Pathways to over 30% efficiency. *Adv Energy Mater*, 2020, 10(13), 1902840
- [6] Helmholtz-Zentrum-Berlin. World record back at HZB: Tandem solar cell achieves 32.5 percent efficiency. 2022
- [7] Yoshikawa K, Kawasaki H, Yoshida W, et al. Silicon heterojunction solar cell with interdigitated back contacts for a photoconversion efficiency over 26%. *Nat Energy*, 2017, 2(5), 17032
- [8] Peibst R, Rienäcker M, Larionova Y, et al. Towards 28%-efficient Si single-junction solar cells with better passivating POLO junctions and photonic crystals. *Sol Energy Mater Sol Cells*, 2022, 238, 111560
- [9] Shockley W. The theory of p-n junctions in semiconductors and p-n junction transistors. *Bell Syst Tech J*, 1949, 28, 435
- [10] Luque A, Hegedus S. Handbook of photovoltaic science and engineering. John Wiley & Sons, 2011
- [11] McIntosh K R. Lumps, Humps and Bumps: Three Detrimental Effects in the Current-Voltage Curve of Silicon Solar Cells. University of New South Wales, 2001
- [12] Bauer A, Hanisch J, Ahlswede E. An effective single solar cell equivalent circuit model for two or more solar cells connected in series. *IEEE J Photovolt*, 2014, 4(1), 340
- [13] Domínguez C, Antón I, Sala G. Multijunction solar cell model for translating I-V characteristics as a function of irradiance, spectrum, and cell temperature. *Prog Photovolt*, 2010, 18(4), 272
- [14] Lang F, Köhnen E, Warby J, et al. Revealing fundamental efficiency limits of monolithic perovskite/silicon tandem photovoltaics through subcell characterization. *ACS Energy Lett*, 2021, 6(11), 3982
- [15] Agarwal Y, Das B, Dutta A J, et al. Numerical simulation of tunneling effect in high-efficiency perovskite/silicon tandem solar cell. *2020 47th IEEE Photovoltaic Specialists Conference (PVSC)*, 2021, 1318
- [16] Blaga C, Christmann G, Boccard M, et al. Palliating the efficiency loss due to shunting in perovskite/silicon tandem solar cells through modifying the resistive properties of the recombination junction. *Sustainable Energy Fuels*, 2021, 5(7), 2036
- [17] Miyano K, Tripathi N, Yanagida M, et al. Lead halide perovskite photovoltaic as a model p-i-n diode. *Acc Chem Res*, 2016, 49, 303
- [18] Velilla E, Cano J, Jimenez K, et al. Numerical analysis to determine reliable one-diode model parameters for perovskite solar cells. *Energies*, 2018, 11(8), 1963
- [19] Cappelletti M A, Casas G A, Cédola A P, et al. Study of the reverse saturation current and series resistance of p-p-n perovskite solar cells using the single and double-diode models. *Superlattices Microstruct*, 2018, 123, 338
- [20] Boccard M, Ballif C. Influence of the subcell properties on the fill factor of two-terminal perovskite-silicon tandem solar cells. *ACS Energy Lett*, 2020, 5(4), 1077
- [21] Tockhorn P, Wagner P, Kegelmann L, et al. Three-terminal perovskite/silicon tandem solar cells with top and interdigitated rear contacts. *ACS Appl Energy Mater*, 2020, 3(2), 1381
- [22] Green M A. Solar cells: operating principles, technology, and system applications. Englewood Cliffs, 1982
- [23] Sah C T, Noyce R N, Shockley W. Carrier generation and recombination in P-N junctions and P-N junction characteristics. *Proc IRE*, 1957, 45(9), 1228
- [24] Henry C H, Logan R A, Merritt F R. The effect of surface recombination on current in $Al_xGa_{1-x}As$ heterojunctions. *J Appl Phys*, 1978, 49(6), 3530
- [25] Fong K C, McIntosh K R, Blakers A W. Accurate series resistance measurement of solar cells. *Prog Photovolt*, 2013, 21(4), 490
- [26] Lin Y R, Yang Z H, Liu Z K, et al. Dual-functional carbon-doped polysilicon films for passivating contact solar cells: Regulating physical contacts while promoting photoelectrical properties. *Energy Environ Sci*, 2021, 14, 6406
- [27] Ying Z Q, Yang X, Zheng J M, et al. Charge-transfer induced multifunctional BCP: Ag complexes for semi-transparent perovskite solar cells with a record fill factor of 80.1%. *J Mater Chem A*, 2021, 9(20), 12009
- [28] Ying Z Q, Yang Z H, Zheng J M, et al. Monolithic perovskite/black-silicon tandems based on tunnel oxide passivated contacts. *Joule*, 2022, 6, 2644
- [29] Shou C H, Zheng J M, Han Q L, et al. Optimization of tunnel-junction for perovskite/tunnel oxide passivated contact (TOPCon) tandem solar cells. *Phys Status Solidi A*, 2021, 218, 2100562
- [30] Green M A, Blakers A W, Osterwald C R. Characterization of high-efficiency silicon solar cells. *J Appl Phys*, 1985, 58(11), 4402
- [31] Saint-Cast P, Werner S, Greulich J, et al. Analysis of the losses of industrial-type PERC solar cells. *Phys Status Solidi A*, 2017, 214(3), 1600708



Yuheng Zeng received his bachelor's and PhD degrees from Zhejiang University. He is a professor at Ningbo Institute of Materials Technology & Engineering (CAS). His research interests include crystalline silicon materials, silicon solar cells, and perovskite/silicon tandem solar cells. He has published more than 100 SCI papers.



Zhenhai Yang received his master and PhD degree from Soochow University and the University of Nottingham (Ningbo), respectively. His research interests include the advanced optical designs, photoelectric models/simulations, structure designs, carrier transport processes, and the related mechanisms for TOP-Con and perovskite-based single/tandem solar cells.



Jichun Ye received his bachelor's and PhD degrees from University of Science and Technology of China and University of California Davis. He has more than 20 years of research and development experience in semiconductor devices, solar cells, and materials and has published more than 220 high-quality papers.